JOURNAL OF VIROLOGY, Nov. 2004, p. 12012–12021 Vol. 78, No. 21
0022-538X/04/$08.00+0 DOI: 10.1128/JVI.78.21.12012–12021.2004

Structural and Thermodynamic Basis for the Binding of TMC114, a Next-Generation Human Immunodeficiency Virus Type 1 Protease Inhibitor

Nancy M. King,[1] Moses Prabu-Jeyabalan,[1] Ellen A. Nalivaika,[1] Piet Wigerinck,[2] Marie-Pierre de Béthune,[2] and Celia A. Schiffer[1]*

Department of Biochemistry and Molecular Pharmacology, University of Massachusetts Medical School, Worcester, Massachusetts,[1] and Tibotec, Mechelen, Belgium[2]

Received 5 March 2004/Accepted 8 June 2004

TMC114, a newly designed human immunodeficiency virus type 1 (HIV-1) protease inhibitor, is extremely potent against both wild-type (wt) and multidrug-resistant (MDR) viruses in vitro as well as in vivo. Although chemically similar to amprenavir (APV), the potency of TMC114 is substantially greater. To examine the basis for this potency, we solved crystal structures of TMC114 complexed with wt HIV-1 protease and TMC114 and APV complexed with an MDR (L63P, V82T, and I84V) protease variant. In addition, we determined the corresponding binding thermodynamics by isothermal titration calorimetry. TMC114 binds approximately 2 orders of magnitude more tightly to the wt enzyme ($K_d = 4.5 \times 10^{-12}$ M) than APV ($K_d = 3.9 \times 10^{-10}$ M). Our X-ray data (resolution ranging from 2.2 to 1.2 Å) reveal strong interactions between the *bis*-tetrahydrofuranyl urethane moiety of TMC114 and main-chain atoms of D29 and D30. These interactions appear largely responsible for TMC114's very favorable binding enthalpy to the wt protease (−12.1 kcal/mol). However, TMC114 binding to the MDR HIV-1 protease is reduced by a factor of 13.3, whereas the APV binding constant is reduced only by a factor of 5.1. However, even with the reduction in binding affinity to the MDR HIV protease, TMC114 still binds with an affinity that is more than 1.5 orders of magnitude tighter than the first-generation inhibitors. Both APV and TMC114 fit predominantly within the substrate envelope, a property that may be associated with decreased susceptibility to drug-resistant mutations relative to that of first-generation inhibitors. Overall, TMC114's potency against MDR viruses is likely a combination of its extremely high affinity and close fit within the substrate envelope.

Human immunodeficiency virus type 1 (HIV-1) protease, a homodimeric enzyme with its active site located at the interface between the two monomers, is responsible for posttranslational processing of the viral Gag and Gag-Pol polyproteins (11). Gag and Gag-Pol are cleaved in at least nine nonhomologous and asymmetric sites (6, 17, 32), releasing both structural proteins and enzymes necessary for viral maturation. Hence, inhibition of HIV-1 protease has been the target of antiviral therapy in patients infected with the virus.

The structural basis for specificity of HIV-1 protease for its substrates has been a focus in our laboratory (33, 35). We solved the crystal structures of an inactive (D25N) variant of the protease in complex with a series of peptides corresponding to the native substrate cleavage sites (35). Analysis of these structures has revealed that binding of the substrate to the enzyme disrupts the symmetry of the protease dimer. In addition, specificity appears to be determined by the asymmetric shape of the substrate rather than by a particular amino acid sequence (35). The region occupied by the substrates, as determined by calculations of their consensus volume, defines what is referred to as a substrate envelope. Structural conservation thus appears to be important (if not essential) for protease-substrate recognition.

* Corresponding author. Mailing address: Department of Biochemistry and Molecular Pharmacology, University of Massachusetts Medical School, 364 Plantation St., Worcester, MA 01605-2324. Phone: (508) 856-8008. Fax: (508) 856-6464. E-mail: Celia.Schiffer@umassmed.edu.

All currently prescribed HIV-1 protease inhibitors, whose structure-based design resulted from extensive investigations of the conformation and function of HIV-1 protease, compete with substrate by binding at the enzyme's active site (44). Although these compounds are chemically different, they occupy a highly overlapping volume, often with similar functional groups positioned at similar locations in the active site. Consequently, atoms of different inhibitors often contact the protease at the same residues. Mutations encoding amino acid substitutions at these regions in the enzyme thus give rise to multidrug-resistant (MDR) viruses, whose mutant proteases no longer bind inhibitors effectively but maintain their ability to recognize and cleave substrates. Due to the rapid replication rate of the virus (7) and the possible infidelity of HIV-1 reverse transcriptase, mutations are generated frequently, thus allowing drug-resistant variants to emerge under the selective pressure of patients undergoing protease inhibitor therapy (9, 36). The generation and transmission of these MDR viruses has created a major challenge for clinicians involved in the treatment of HIV infection.

Examination of the Stanford HIV Drug Resistance Database of HIV-1 infected-patient sequences of viral isolates (http://hivdb.stanford.edu) reveals certain patterns of mutational selection occurring with different protease inhibitor treatments (39, 40). When we analyzed and compared these patterns to the active-site regions occupied by the inhibitors, we found that the primary drug-resistant mutations often occurred at positions in the protease that are contacted by inhib-

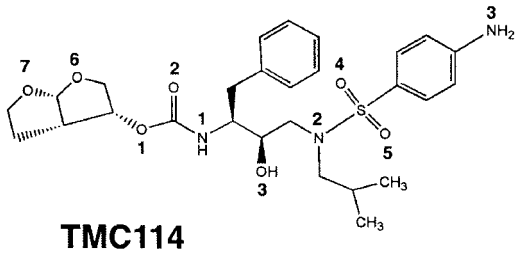

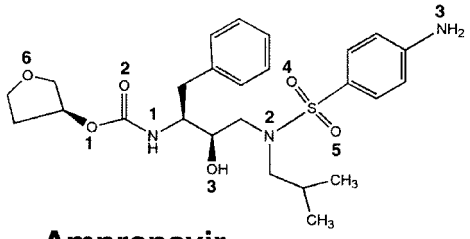

FIG. 1. The chemical structures of APV and TMC114.

itor atoms protruding beyond the volume of the substrate envelope (20a). Of the five protease inhibitors that have been prescribed for more than 1 year, amprenavir (APV) is the only compound that fits predominately within this envelope. This unique property of APV likely explains its pattern of selecting viral mutants and drug resistance in patient viral isolates, which is somewhat different than that of first-generation inhibitors.

APV binding to the wild-type (wt) protease is tighter by about 1 order of magnitude than that of the first-generation inhibitors: indinavir, nelfinavir, saquinavir, and ritonavir (43). Thermodynamic studies have shown that APV binding is both enthalpically and entropically favorable, whereas binding of the above-mentioned inhibitors is mainly entropically driven (42). These unique properties of APV could provide a template for the development of new tightly binding HIV-1 protease inhibitors. In fact, the single-ringed tetrahydrofuran (THF) group of APV was replaced with a double-ringed *bis*-THF to design a protease inhibitor with an enhanced enthalpy change (16, 45). However, this inhibitor, TMC126, in which the carboxymethyl moiety substitutes for the four-amino group on the aryl sulfonamide, lacked sufficient drug-like properties such as solubility, metabolic stability, and oral absorption to be a viable lead.

Work with TMC126, however, led to the selection of the clinical candidate TMC114, a protease inhibitor that is chemically related to both TMC126 and APV (Fig. 1) and is highly potent against a wide range of drug-resistant viruses in vitro. The 50% effective concentration of TMC114 against wt HIV is 4.6 nM, with a selectivity index greater than 20,000 (10). When compared with currently prescribed protease inhibitors, TMC114 was substantially more active against over 1,600 protease-inhibitor-resistant clinical isolates (12). In a phase IIa clinical trial, TMC114 boosted with ritonavir replaced a failing protease regime in HIV-infected patients. After 14 days on this functional monotherapy regime, these patients showed a median 1.35-log drop in viral load (2). Despite its minimal chemical difference from APV, TMC114 was thus shown to perform significantly better against drug-resistant viral isolates.

Our laboratory has used a MDR protease variant having the amino acid substitutions L63P, V82T, and I84V (Fig. 2), for which we have shown has weaker binding affinity to all of the first-generation inhibitors in clinical use (N. M. King, unpublished data), including APV. The substitutions at positions 82 and 84 affect the polarity and geometry, respectively, of the active site. The mutation of I84V has the largest impact on inhibitor binding, affecting all prescribed protease inhibitors. The mutation L63P, located in the hinge region of the protein, away from the active site, has been shown to compensate for active-site mutations, restoring the impaired catalytic activity of the enzyme (22, 38). Thus, this triple-mutant variant is a useful prototype for studying MDR in HIV-1 protease.

In the present study, we determine and compare the X-ray crystallographic structures and thermodynamics of APV and TMC114 binding to the wt HIV-1 protease and our MDR prototype variant. Detailed analyses of the structures of these two inhibitors in complex with both proteases are used to explain the reasons for differences in binding affinities as determined by isothermal titration calorimetry. APV and TMC114 binding are both shown to be enthalpically and entropically driven, with TMC114 binding approximately 2 orders of magnitude more tightly than APV. The three-dimensional structures of these complexes reveal hydrogen bonds between TMC114 and the protease that are not seen in the APV wt complex. These additional hydrogen bonds may partially explain the extremely favorable enthalpy of binding for TMC114

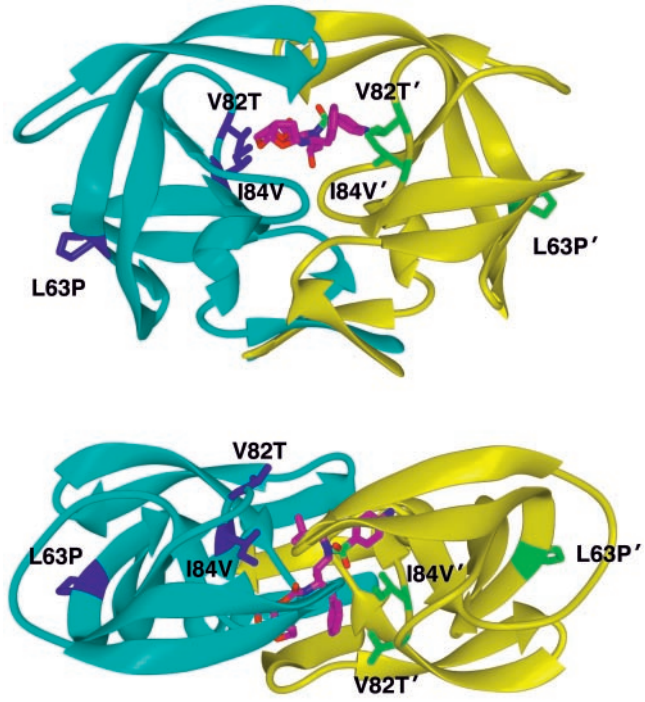

FIG. 2. Two orientations of the $TMC114_{3X}$ protease complex, shown as ribbon diagrams. The two monomers of HIV protease are shown in cyan and yellow with the side chains of the sites of mutation shown, labeled, and highlighted in blue and green. TMC114 is shown in magenta (15).

compared to APV. In addition, both compounds are located predominantly within the substrate envelope, which may account in part for the decreased susceptibility to existing drug-resistant protease variants. Our analysis of the structural and thermodynamic properties of these two inhibitors should provide insights for designing the next generation of inhibitors with enhanced binding affinity to the wt enzyme and improved efficacy against MDR viruses.

MATERIALS AND METHODS

Nomenclature. HIV-1 protease variants (wt or MDR [3X]) will be distinguished throughout this article by subscript acronyms. For example, $TMC114_{wt}$ denotes a complex of the inhibitor TMC114 with the wt protease. Primes are used to distinguish the two monomers in the protease dimer.

Protease gene construction. The MDR protease gene coding for the substitutions L63P, V82T, and I84V was constructed using standard site-directed mutagenesis of a synthetic protease variant (20). The synthetic protease also encoded the Q7K substitution to prevent autoproteolysis (37).

Protein expression and purification. The protease was expressed and purified as previously described (20). The protein was refolded by rapid dilution in a 10-fold volume of 0.05 M sodium acetate buffer at pH 5.5, containing 10% glycerol, 5% ethylene glycol, and 5 mM dithiothreitol (refolding buffer). To reduce the volume, the protease was concentrated, followed by dialysis to remove any remaining acetic acid. Protease used for crystallization was further purified with a Pharmacia Superdex 75 fast-performance liquid chromatography column equilibrated with refolding buffer.

Crystallization. Crystals were set up with a three- to fivefold molar excess of inhibitor to protease, which ensures ubiquitous binding. The final protein concentration ranged from 0.5 to 2.5 mg ml^{-1} in refolding buffer. The hanging-drop method was used for crystallization as previously described (20). The reservoir solution consisted of 126 mM phosphate buffer at pH 6.2, 63 mM sodium citrate, and ammonium sulfate at a range of 25 to 33%.

Data collection. Data on the $TMC114_{3X}$ and $TMC114_{wt}$ complexes were collected under cryocooled conditions with the synchrotron source at Advanced Light Source at Lawrence-Berkeley National Laboratory, Berkeley, Calif. The crystals were screened using robotics available at the 5.0.2 beam line. About 200 frames were collected from the best diffracting crystals, with each frame exposed for 30 s and the wavelength tuned to 0.9 Å. Data for the APV_{3X} complex were collected at room temperature, as the crystals were too large to freeze efficiently. Crystals were mounted inside 0.3-mm-diameter capillary tubes, and data were collected on an R-axis IV image plate system mounted on a Rigaku rotating anode source. Two hundred frames were collected for this complex at 1-degree intervals, with each frame exposed for 4 min. Denzo and ScalePack (23, 30) were used to integrate and scale the raw data frames for all three complexes. Data collection statistics are listed in Table 1.

Structure solution and crystallographic refinement. The method described in Prabu-Jeyabalan et al. (34, 35) was used to solve and refine the APV_{3X} complex. The Fourier synthesis method was used for structure solution, with the substrate structure, 1F7A, as the starting model. Structures were refined using the Crystallography & NMR system (4). Refinement statistics for APV_{3X} are given in Table 1. For the TMC114 complexes, however, CCP4i (8) was used for all crystallographic calculations. Structure solutions were obtained with the molecular replacement package AMoRe (27), with 1F7A as the starting model. A radius of integration of 20 Å and X-ray data within 4.0 to 2.5 Å were used for the structure solution. Rigid body refinement was then carried out with Refmac5 (26), followed by initial-phase improvement to extend the entire data set with the water-picking program ARP/wARP (24). Difference Fourier maps were computed and inspected with the interactive graphic program O (18), and major structural changes in the model, such as the inclusion of the inhibitor, were incorporated. After manual model building, the real space refinement package RSREF (5) was used to fine-tune the fit between the model and electron density maps. After every RSREF run, restrained refinement with Refmac5 was undertaken. Finally, crystallographic anisotropic temperature factors were refined. The final refinement statistics are listed in Table 1.

Isothermal titration calorimetry. Thermodynamic parameters of inhibitor binding were determined using an isothermal titration calorimeter, VP-ITC (MicroCal Inc., Northampton, Mass.). The buffer used for all protease and inhibitor solutions consisted of 10 mM sodium acetate (pH 5.0), 2% dimethyl sulfoxide, and 2 mM Tris (2-carboxyethyl) phosphine. The binding affinities of APV and TMC114 for both the wt and MDR proteases were obtained by the displacement titration method, with either acetyl-pepstatin or indinavir as the weaker binder (29, 41, 43). Indinavir (75 to 200 μM) was used exclusively in competition experiments with the mutant protease (6.3 to 11.5 μM) and TMC114 (78 to 83 μM). Pepstatin (250 to 300 μM) provided the competing inhibitor for all other assays, with a protease concentration of 15.6 to 22 μM. For all displacement experiments with wt protease, TMC114 and APV were used at concentrations of 56 and 250 μM, respectively. Twenty injections (each, 10 μl) of the weak binder were injected into the calorimetric cell containing the protease, followed by 29 injections (each, 10 μl) of the tight binder. Direct titration experiments were also performed with the tightly binding inhibitor to confirm the enthalpy changes obtained by the displacement method. Each experiment was performed at least twice. Heats of dilution were subtracted from the corresponding heats of reaction to obtain the heat due solely to inhibitor binding to the enzyme. Data were processed using software kindly provided by B. Sigurskjold (41).

TABLE 1. X-ray crystallographic data collection and refinement statistics for the three inhibitor-protease complexes

Variable	Complex		
	$TMC114_{wt}$	$TMC114_{3X}$	APV_{3X}
Resolution (Å)	1.20	1.35	2.20
Temperature (°C)	−80	−80	25
Mirror	LBL[a]	LBL[a]	Osmic
Space group	$P2_12_12_1$	$P2_12_12_1$	$P2_12_12_1$
a (Å)	50.746	50.858	51.070
b (Å)	57.807	58.040	59.342
c (Å)	62.006	61.656	61.823
Z	4	4	4
R_{merge} (%)	3.8	4.4	8.7
Completeness (%)	95.5	98.0	96.8
Total no. of reflections	302,022	256,671	49,950
No. of unique reflections	55,056	39,998	9,705
R_{factor} (%)	14.1	16.8	20.3
R_{free} (%)	17.9	20.0	24.4
No. of crystallographic waters	263	203	58
RMSD[b] in:			
Bond lengths (Å)	0.004	0.005	0.007
Bond angles (°)	1.50	1.30	1.38
B factors (isotropic) RMSD bonded ($Å^2$)			
Main chain	1.5	1.5	1.7
Side chain	3.0	3.0	2.9
I/σI	25.0	13.5	5.9
PDB code[c]	1T3R	1T7I	1T7J

[a] Data collected at Advanced Light Source, Lawrence-Berkeley National Laboratory.
[b] RMSD, root mean square deviation.
[c] PDB, Protein Data Bank.

RESULTS

Overall structural features. The MDR HIV-1 protease variant with substitutions L63P, V82T, and I84V was crystallized in complex with two inhibitors, APV and TMC114 (referred to as APV_{3X} and $TMC114_{3X}$ complexes, respectively). The wt protease was crystallized in complex with TMC114 only (referred to as $TMC114_{wt}$), since the APV_{wt} structure has already been solved (Protein Data Bank entry 1HPV) (19). Crystallographic statistics for these structures are listed in Table 1. The TMC114 structures and APV_{3X} crystallized in the space group $P2_12_12_1$, with similar cell dimensions and one dimer per asymmetric unit. The APV_{wt} structure is in the $P6_1$ space group, also with one dimer per asymmetric unit and a resolution of 1.9 Å (19). Any deviations between structures arising as a result of different crystal contacts are accounted for in the present analysis.

As shown in Table 1, the present structures were refined to resolutions ranging from 2.2 to 1.2 Å. The electron density for all inhibitor and protease atoms was well ordered in each of the

three structures. The mutated side chains also showed unambiguous electron density, with two different conformations clearly demonstrated in some cases (see below). Contrary to most of the previous structures of complexes between the protease and first-generation inhibitors solved in our laboratory, no alternate conformations were observed for residues I50 and G51 located at the tips of the flaps (20; King, unpublished). Minor structural adjustments due to the different inhibitors bound in the active site or to mutations in the protease were identified between complexes and will be described below.

$TMC114_{wt}$ complex. The complex between the wt protease and the tightly binding inhibitor TMC114 was refined to high resolution (1.20 Å), allowing a very detailed structural analysis. The R_{factor} for this complex was 14.1%, with 263 water molecules clearly defined. The inhibitor had strong electron density and was uniquely modeled in one conformation. Alternate conformations were observed for active-site residues I47, V82, V32′, and V82′. Two conformations were also observed for residues L19, E21, C95, M46′, and E65′.

$TMC114_{3X}$ complex. The crystal complex between the MDR HIV protease variant and TMC114 diffracted to a resolution of 1.35 Å, with an R_{factor} value of 16.8%. Protease residues that were present in two conformations and within van der Waals distance of the inhibitor molecule included R8 and T82 from both monomers, as well as I47 and L23′. Nine additional residues located outside of the active site also had two conformations.

APV_{3X} complex. Data for the APV_{3X} complex were collected with our local instrumentation at room temperature, and therefore its resolution is somewhat less than that of the TMC114 complexes. However, the APV_{3X} structure's resolution of 2.2 Å was sufficient for comparison with the other structures. The inhibitor molecule was modeled in one conformation, except for its *N*-isobutyl group, which has two orientations. The χ_2 angle in one conformer is 53° and −131° in the other. All residues in the active-site region were uniquely modeled in one conformation, indicating stability in this area of the complex. However, two conformations were observed for residues I15, Q18, E34, E35, and I64 and for residues N37′, M46′, and I64′, all located outside the inhibitor binding site.

Structural comparisons between wt complexes. Important differences were observed in hydrogen-bonding patterns between the $TMC114_{wt}$ and APV_{wt} structures. Figure 3 shows hydrogen bonding between atoms in the protease active site and atoms in the inhibitor, including those mediated by water. A highly conserved water molecule tetrahedrally coordinated the backbone nitrogen atoms in I50 of both monomers at the tips of the flaps to O2 and O5 of the inhibitors. Replacement of the single-ringed THF group in APV with the double-ringed *bis*-THF group in TMC114 (Fig. 1) resulted in additional hydrogen bonds in the $TMC114_{wt}$ complex not seen in the APV_{wt} structure. As seen in Table 2 and Fig. 3c, the O7 oxygen in the added ring of TMC114 was within hydrogen-bonding distance of both the backbone nitrogen (2.9 Å) and one of the carboxyl oxygens (3.3 Å) of D29. Furthermore, this added ring appeared to pull that end of the inhibitor molecule closer to that region of the active site.

The most significant differences between the wt protease complexes with APV and TMC114 were in the lengths of the hydrogen bonds with the protease. The largest differences were between the O6 oxygen of the inhibitors and the backbone nitrogens of residues D29 and D30 and between the N1 nitrogen of the inhibitors and the backbone oxygen of G27 (Table 2 and Fig. 3). In the $TMC114_{wt}$ complex (Fig. 3a), these distances were all 3.1 Å for D29, D30, and G27, whereas in the APV_{wt} complex (Fig. 3b) the corresponding distances were 3.5, 3.5, and 3.6 Å, too far to easily form strong hydrogen bonds. At the other side of the active-site cleft, an additional hydrogen bond was evident in the $TMC114_{wt}$ complex: the N3 nitrogen of TMC114 was 3.1 Å from the carbonyl oxygen of D30′, whereas the corresponding distance was 3.6 Å in the APV_{wt} structure. Thus, at least six hydrogen bonds occurred between the wt protease and TMC114, but not APV, likely resulting in the $TMC114_{wt}$ complex being more stable than the APV_{wt} complex. This is evident in Fig. 3c, where the two wt complexes are superimposed; TMC114 is shifted slightly relative to APV, allowing TMC114 to form more and tighter hydrogen bonds. In addition, most of the hydrogen-bonding interactions between TMC114 and the protease involved main-chain atoms located at the bottom of the active-site cleft, thus decreasing the effects of mutations occurring in that region of the protease.

Structural comparison between the wt and MDR complexes. Flexibility in both proteins and ligands appeared to compensate for any potential reduction in interactions resulting from the mutations. For example, the rotatable bond of the *N*-isobutyl group in TMC114 and APV allowed for conformational adjustments in the ligand. This flexibility is beneficial for the inhibitor, since this moiety faces residue 84 in the active site, a common site of drug-resistant mutation. Different orientations of the *N*-isobutyl group can be seen in the four complexes (Fig. 4): in the two TMC114 structures, the *N*-isobutyl group has the same orientation, which differs from those in each APV structure. This group is within 4.2 Å of I84 in $TMC114_{wt}$ and thus makes van der Waals contacts (Fig. 4a). These interactions are reduced, however, in APV_{wt} where the *N*-isobutyl group is rotated around χ_1 (Fig. 4b). A loss in van der Waals interactions was also seen in the $TMC114_{3X}$ structure, where the I84V substitution changed the volume and geometry of the active site (Fig. 4c). In the second monomer, however, the side chain of V84 underwent a rotation around χ_1, at least partially filling this gap. The APV_{3X} complex did not appear to have suffered as great a loss in van der Waals interactions, since the *N*-isobutyl group took on two conformations, thus maintaining these interactions with V84 (Fig. 4d). In the second monomer, the interactions with residue 84 were primarily maintained, due to the shift and tilt in APV's position in the active site (Fig. 4f).

The positions of the loop regions between residues 79 and 81 (the 80s loops) in the protease active site sometimes change between structures, due to relative shifts and tilts in the bound ligand (1, 3, 20, 25). We have observed these changes between both wt structures and their corresponding mutant complexes. The shift of the ligand in $TMC114_{3X}$ by an average of 0.16 Å relative to its position in the wt structure coincided with a repositioning of the 80s loop of one monomer (Fig. 4e), but very little change was observed in the same region of the other monomer. The shift and tilt of APV in the mutant structure relative to the wt complex paralleled the shift of both 80s loops (Fig. 4f). The positions of the inhibitor in APV_{wt} and in APV_{3X} differed by an average of 0.34 Å and an average angle of 6.25°. With this repositioning of the ligand, the 80s loop in one

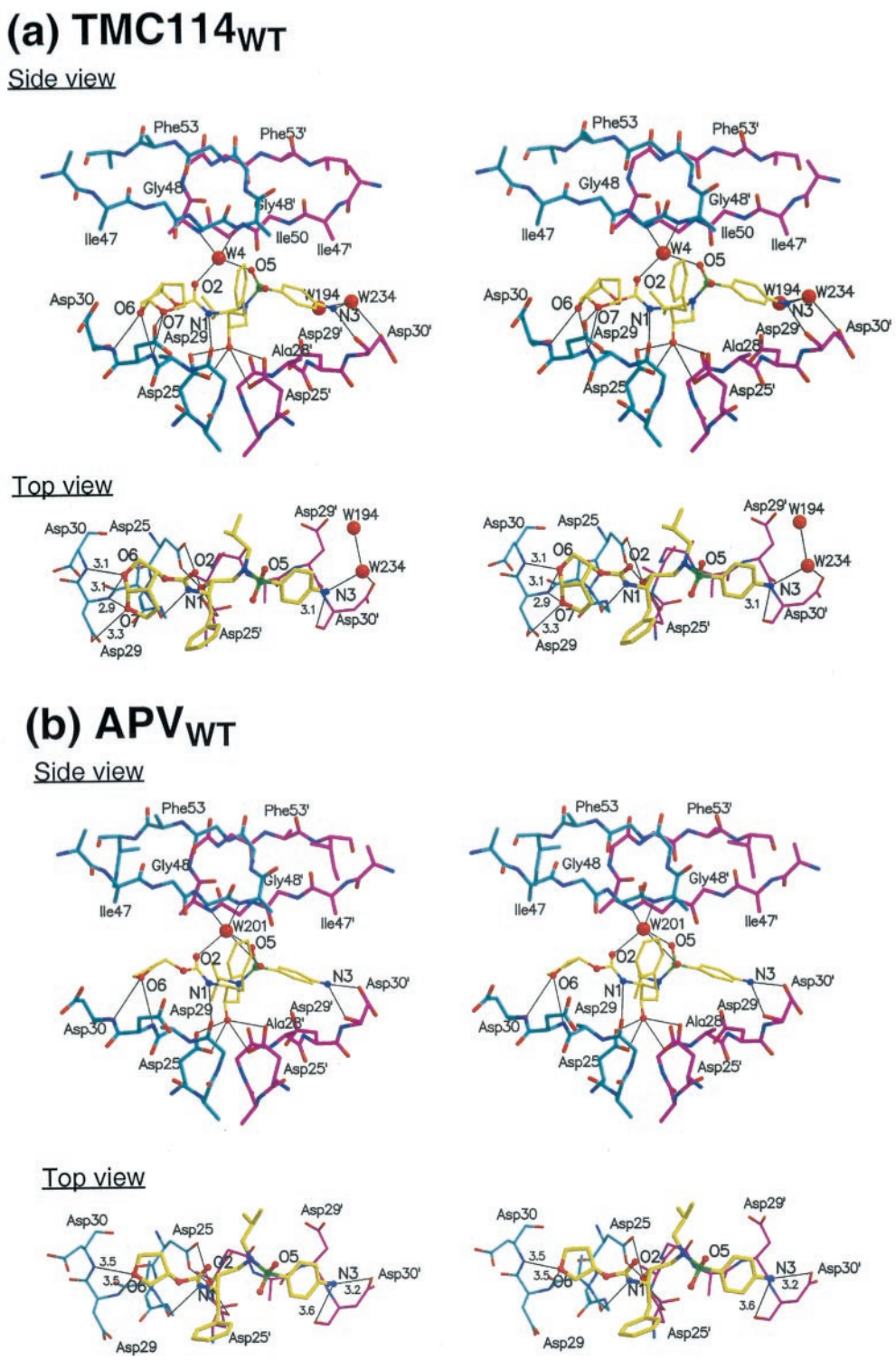

FIG. 3. Stereo pairs showing the network of hydrogen bonds between (a) the $TMC114_{wt}$ complex (note that the hydrogen bonds are the same between the wt and MDR protease complexes with TMC114) (Table 2), (b) the APV_{wt} complex, (c) superimposition of $TMC114_{wt}$ (in magenta and purple with hydrogen bonds in black) and APV_{wt} (in cyan and gray with hydrogen bonds in yellow), and (d) the APV_{3X} complex (15).

monomer moved towards the inhibitor, whereas the same region in the other monomer moved away. Thus, the 80s loops adjusted to each of the inhibitors, depending on the specific interactions within that complex.

The locations and lengths of hydrogen bonds between the inhibitor and protease in the $TMC114_{3X}$ complex were very similar to those for the $TMC114_{wt}$ structure (Table 2). Although the ligand's position shifted slightly within the active

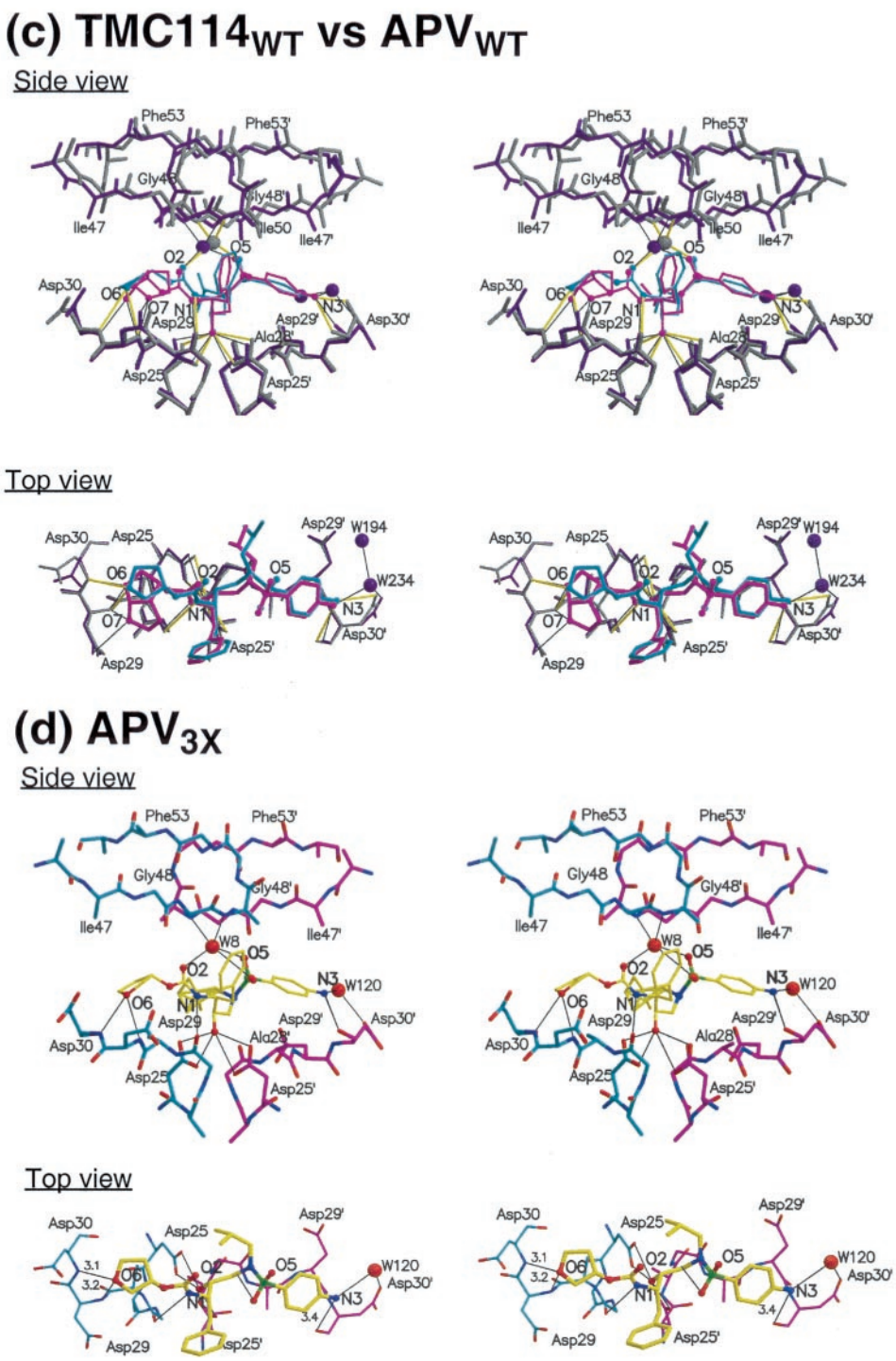

FIG. 3—*Continued.*

site of the $TMC114_{3X}$ structure (Fig. 4e), this shift was not sufficient to disrupt these interactions. In addition, a new interaction was seen between protease and inhibitor in the $TMC114_{3X}$ complex. One of the conformations of T82 was oriented such that it made OH-π interactions with the phenyl ring of the inhibitor. However, the T82 side chain in APV_{3X} points away from the inhibitor (Fig. 4f) and thus did not interact with APV's phenyl ring, as in the $TMC114_{3X}$ structure (Fig. 4e). Otherwise, as shown in Table 2 and Fig. 3d, the hydrogen-bonding pattern for the APV_{3X} complex more closely resembled that of the TMC114 complexes than the APV_{wt} complex. Rearrangements in the APV_{3X} complex resulted in closer hydrogen bonds between ligand and active-site atoms than in the APV_{wt} structure. In APV_{3X}, the O6 oxygen of APV was 3.2 and 3.1 Å from the amide nitrogens of D29 and D30, respectively. In the APV_{wt} structure, on the other hand, these

TABLE 2. Hydrogen-bonding distances between protease and inhibitor atoms in APV and TMC114 structures

Protease atom	Inhibitor atom	Distance (Å) for:			
		$TMC114_{wt}$	$TMC114_{3X}$	APV_{wt}	APV_{3X}
Asp 29 N	O6	3.1	3.1	3.5	3.2
Asp 30 N	O6	3.1	3.1	3.5	3.1
Asp 29 N	O7	2.9	2.9		
Asp 29 OD2	O7	3.3	3.3		
Water	O2	2.8 (W4)[a]	2.8 (W2)	3.0 (W201)	2.8 (W8)
Gly 27 O	N1	3.1	3.1	3.6	3.5
Asp 25′ OD1	O3	3.0	2.5	2.7	2.6
Asp 25′ OD2	O3	2.5	2.9	2.8	3.1
Asp 25 OD1	O3	2.6	2.6	2.6	2.7
Asp 25 OD2	O3	3.3	3.2	3.1	2.9
Water	O5	2.9 (W4)	2.8 (W2)	2.8 (W201)	2.9 (W8)
Water	O4			3.4 (W201)	3.4 (W8)
Asp 30′O	N3	3.1	3.2	3.6	3.3
Water	N3	3.0 (W234)	2.9 (W86)		3.4 (W120)
Asp 30′ OD2	N3			3.2	

[a]The corresponding water number is in parentheses.

distances were both 3.5 Å, which are long and therefore weak for hydrogen bonds. The tilt in the ligand of the APV_{3X} structure relative to its position in the APV_{wt} complex (Fig. 4f) was also demonstrated in the distance between the N3 nitrogen of APV and the main-chain oxygen atom of D30′ at the other side of the active-site cleft. The N3 nitrogen was closer to the carbonyl oxygen (3.3 Å) in APV_{3X} than in APV_{wt} (3.6 Å) (Table 2 and Fig. 3d). The N3 nitrogen end of the ligand was farther away from the primed monomer in the APV_{wt} structure than in the APV_{3X} complex. Thus, adjustments demonstrated in the MDR APV_{3X} complex were not seen when TMC114 was bound in the active site.

Comparison with the substrate envelope. Our laboratory has hypothesized that HIV-1 protease recognizes an asymmetric shape, or envelope, adopted by its substrates rather than a particular amino acid sequence (35). If the substrate envelope was superimposed on the inhibitor structures of TMC114 and APV, only a few atoms of each inhibitor protruded beyond the envelope (Fig. 5). Residues 25, 27, 28, 29, and 30 were all located at the bottom of the active-site cleft, and residues 47, 49, and 50 were in the flaps at the top of the active site. Residues 32 and 84 are located on both sides of the active site. These residues represent potential sites where drug-resistant mutations impacting TMC114 and APV could occur.

Thermodynamics. Isothermal titration calorimetry was used to determine the thermodynamics of binding between the wt

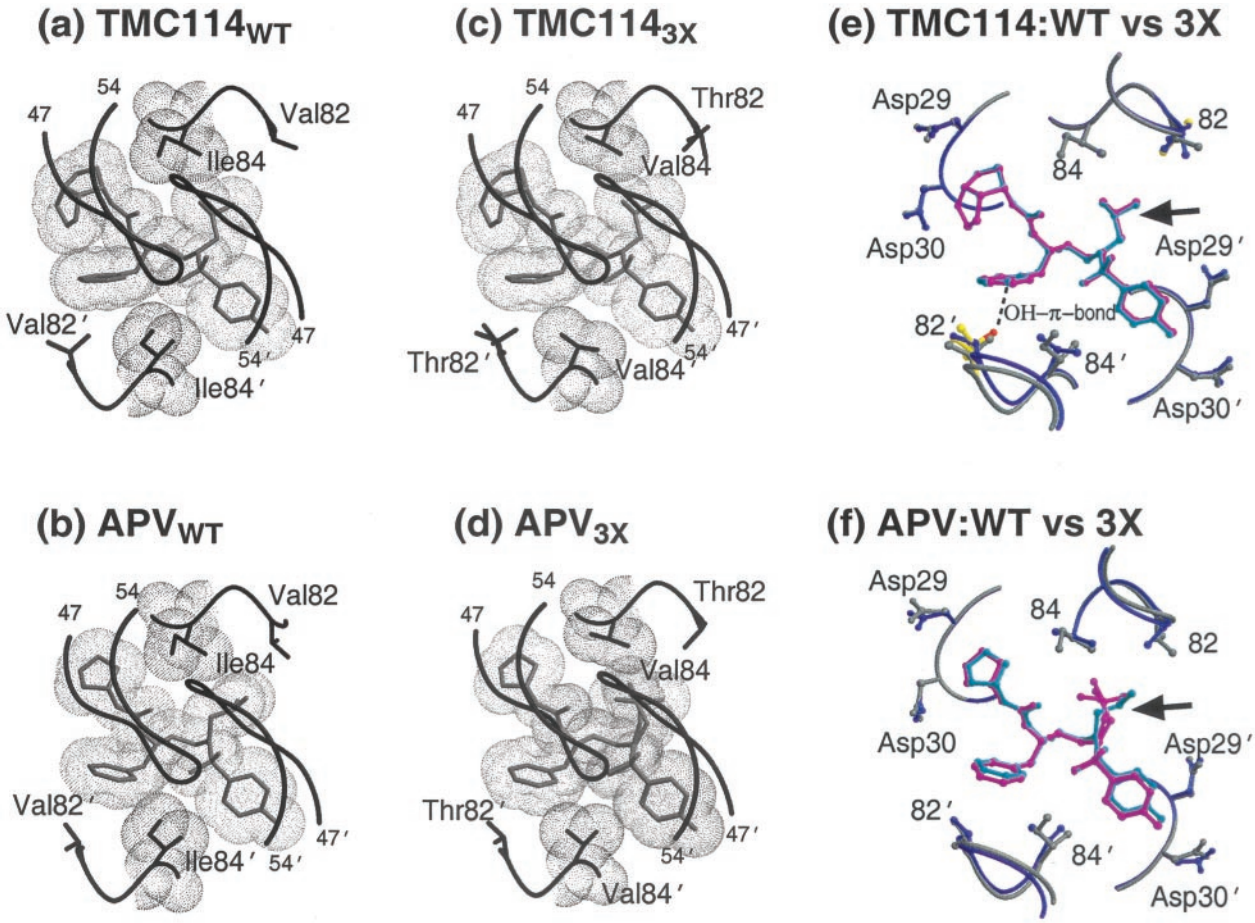

FIG. 4. Inhibitor interactions with residues 82 and 84 in the various protease complexes (15). (a) $TMC114_{wt}$ complex showing the van der Waals interactions between TMC114 and I84. (b) APV_{wt} complex showing the van der Waals interactions between APV and I84. (c) $TMC114_{3X}$ complex showing the van der Waals interactions between TMC114 and V84. (d) APV_{3X} complex showing the van der Waals interactions with V84. (e) Superposition of $TMC114_{wt}$ (in gray and cyan) and $TMC114_{3X}$ (in purple-yellow and magenta) complexes. Note the additional OH-π hydrogen bond made by T82. (f) Superposition of APV_{wt} and APV_{3X} complexes. Note the conformational variability of the *N*-isobutyl group (arrow).

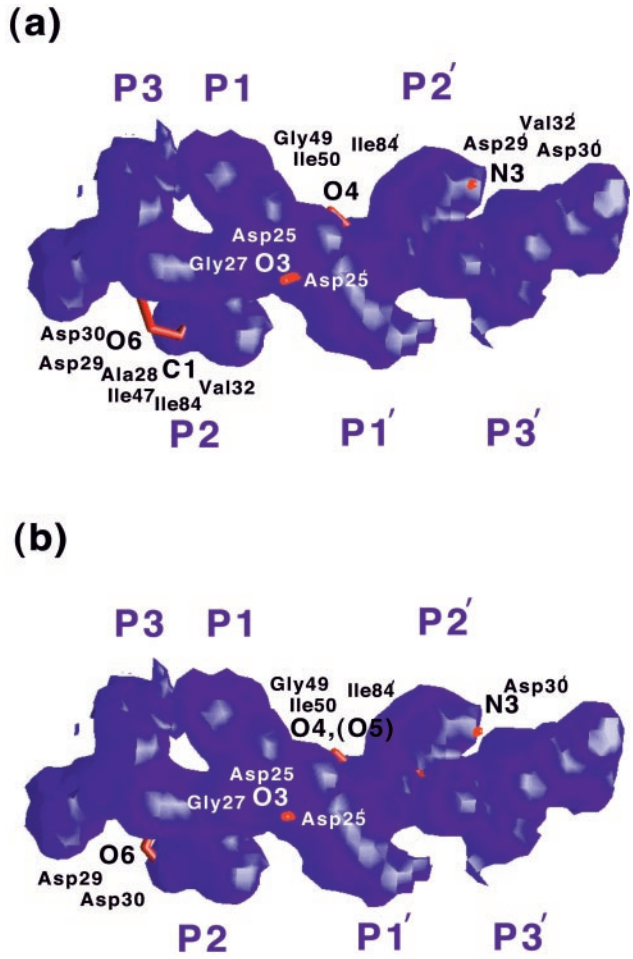

FIG. 5. Substrate envelope (35) of HIV protease shown in blue (28), superimposed on the structures of (a) TMC114 and (b) APV. The atoms of each of the inhibitors that protrude from the envelope are shown in red and labeled. HIV protease residues that are within van der Waals contact of these atoms are also labeled.

and MDR proteases and the inhibitors APV and TMC114. Table 3 lists the thermodynamic parameters of binding for each protease-inhibitor pair. Both inhibitors bound with favorable enthalpy and entropy changes, with the enthalpic contribution being particularly high for TMC114's binding to the wt enzyme ($\Delta H = -12.1$ kcal/mol $-T\Delta S = -3.1$ kcal/mol). The change in free energy resulted in tight binding of both inhibitors, as indicated by dissociation constants of 3.9×10^{-10} M and 4.5×10^{-12} M for APV and TMC114, respectively. As shown in Table 3, the binding constant for TMC114 to the wt protease was approximately 87-fold greater than APV, with a difference in binding enthalpy of 4.8 kcal/mol. Thus, the binding of TMC114 to the wt protease was more enthalpically driven than binding of APV. For the binding of APV, the enthalpic and entropic contributions to the total free energy of binding were more similar ($\Delta H = -7.3$ kcal/mol; $-T\Delta S = -5.3$ kcal/mol). The loss of favorable entropy by 2.2 kcal/mol for TMC114 relative to APV, the underlying basis of which is not clear, was compensated for by the significantly more-favorable enthalpy change of 4.8 kcal/mol. Thus, enthalpy appeared to drive the increased binding affinity of TMC114.

TMC114 binding to the MDR 3X mutant protease was 13.3 times less tight than its binding to the wt enzyme. Although the enthalpy change is less favorable by 2.1 kcal/mol, the entropic contribution becomes slightly more favorable ($\Delta - T\Delta S = -0.6$ kcal/mol). APV binding to the mutant protease is less compromised than that of TMC114 (Table 3); the ratio of binding affinities for APV ($K_{d\ 3X}/K_{d\ wt}$) is 5.1, with nearly equivalent losses in enthalpic (0.3 kcal/mol) and entropic (0.6 kcal/mol) contributions to free energy. The I84V substitution in the mutant protease, which reduces van der Waals interactions with the inhibitor, is likely the main reason for the reduced binding affinity of both APV_{3X} and $TMC114_{3X}$ (Fig. 4). The I84V substitution had less of an effect on the binding of APV, mainly because of the strong interactions with D29 and D30 in this complex. These interactions compensated for some of the loss in van der Waals interactions. This observation also supports the importance of these interactions in increasing binding affinity. However, although TMC114 lost a larger percentage of

TABLE 3. Binding thermodynamics of APV and TMC114 at 20°C

Pair	K_a (M^{-1})	K_d (M)	ΔH (kcal/mol)	$-T\Delta S$ (kcal/mol)	ΔG (kcal/mol)
Wild type					
APV	2.5×10^9	3.9×10^{-10}	−7.3	−5.3	−12.6
TMC114	2.2×10^{11}	4.5×10^{-12}	−12.1	−3.1	−15.2
		$K_{dAPV}/K_{d\ TMC114}$	ΔΔH (kcal/mol)	Δ−TΔS (kcal/mol)	ΔΔG (kcal/mol)
		86.7	4.8	−2.2	2.6
3x Mutant		K_d (M)	ΔH (kcal/mol)	$-T\Delta S$ (kcal/mol)	ΔG (kcal/mol)
APV	5.1×10^8	2.0×10^{-9}	−7.0	−4.7	−11.7
TMC114	1.7×10^{10}	6.0×10^{-11}	−10.0	−3.7	−13.7
		$K_{dAPV}/K_{dTMC114}$	ΔΔH (kcal/mol)	Δ−TΔS (kcal/mol)	ΔΔG (kcal/mol)
		33.3	3.0	−1.0	2.0
		$K_{d3\times}/K_{dwt}$	ΔΔH (kcal/mol)	Δ−TΔS (kcal/mol)	ΔΔG (kcal/mol)
APV		5.1	0.3	0.6	0.9
TMC114		13.3	2.1	−0.6	1.5

its total binding affinity, it still bound more than 33-fold tighter to the MDR protease than did APV.

DISCUSSION

Our analyses of the binding and structure of the HIV-1 protease inhibitors APV and TMC114 provide a rationale for the potency that renders them more advantageous than the first-generation inhibitors. Both compounds bind to the protease with high affinity, yet TMC114 is a particularly tight binder, due to additional strong interactions with main-chain atoms at the bottom of the active site. TMC114 binding is mainly enthalpically driven, whereas the enthalpic and entropic contributions to the binding of APV are nearly equivalent. TMC114 binds almost 2 orders of magnitude more tightly than APV but protrudes further from the substrate envelope. This protrusion allows TMC114 to form more hydrogen bonds, which likely increase its affinity for the protease. Yet, those same protruding atoms may cause it to take a more substantial decrease in its binding constant when it binds to drug-resistant variants. However, since TMC114 already starts with an extremely tight affinity, it can sustain a substantial decrease in its binding constant without compromising its activity, allowing it to remain effective.

In a modeling study of APV and the closely related HIV-1 protease inhibitor TMC126 (29), Ohtaka et al. attribute the highly favorable binding enthalpy of TMC126 to strong interactions and sequestered water molecules. The strong interactions found between TMC126 and D29 and D30 at the bottom of the active-site cleft agree with our analyses of X-ray structures of TMC114. We found an additional hydrogen-bonding interaction with the backbone carbonyl oxygen of G27, which is not seen in the wt APV structure. Furthermore, the more-favorable binding enthalpy of TMC126 was attributed to its ability to sequester more water molecules than APV (29). Our high-resolution X-ray crystallographic structures did not, however, reveal a significantly different number of water molecules at the binding sites of the TMC114, suggesting that sequestration of water molecules may not contribute to the highly favorable enthalpy change for the binding of TMC114. Strong, direct protease inhibitor interactions therefore likely contribute predominantly to the very high binding affinity of this inhibitor.

TMC114 and APV fit within the substrate envelope better than any currently prescribed protease inhibitor. HIV-1 protease residues that are contacted by an inhibitor at sites where it protrudes from the substrate envelope are potential sites of drug-resistant mutations. For TMC114, these residues include G27, A28, D29, D30, V32, I47, I50, and I84. Several of these residues, G27, A28, and D29, have never or rarely been seen to mutate in the current Stanford HIV Drug Resistance Database (http://hivdb.stanford.edu) (39, 40). In vitro studies have shown that the closely related HIV-1 protease inhibitor TMC126 selects for active-site mutations at A28 and I50, as well as for mutations remote from the active site (45). Alanine at position 28 in HIV-1 protease is highly conserved; substitution at A28 occurred in only four of 6,099 HIV-1 infected patients (39, 40; http://hivdb.stanford.edu). Since TMC114 and TMC126 are so similar in structure, they are likely to have the same fit in the active site and to contact the same protease residues. Thus, although TMC114 contacts such commonly mutating protease residues as D30, V32, I47, I50, and I84, mutations at these sites have so far not been selected in vitro when wt HIV-1 is exposed to increasing concentrations of inhibitor (13). However, studies are under way to investigate the susceptibility to TMC114 of viruses having preexisting protease mutations. APV, on the other hand, with its slightly different binding mode and lower binding affinity, does in fact select in vitro for active-site mutations at I47, I50, and I84 (31).

Since TMC114 binds so tightly, the simultaneous occurrence of multiple mutations at several of these sites may be necessary before the virus becomes resistant to the inhibitor. However, if TMC114 effectively suppresses viral turnover, the opportunity for selection of resistance will be greatly decreased. If resistant variants arise which have multiple mutations, substrate binding may also be affected. The further evolution of substrate sites would be required for the virus to survive. Such coevolution has occasionally been seen, although it has been primarily limited to the NC-p1 cleavage site. In this case, the P2 residue mutates from an alanine to a valine in the presence of the V82A protease drug-resistant mutation (14, 21, 46). These results are encouraging in that the virus may have more difficulty in developing resistance to TMC114 than to other protease inhibitors; however, with the heterogeneity of HIV in vivo this will be confirmed only when extensive clinical trials are concluded.

Our findings suggest that the potency of TMC114 is due to a combination of two factors: (i) its extremely tight binding (K_d = 4.5 pM) and (ii) its close fit within the substrate envelope. The promise of TMC114 as a next-generation protease inhibitor is supported by our structural and thermodynamic analyses of its unique properties, which provide a framework for the design of new inhibitors exhibiting potency on both wt and MDR viruses.

ACKNOWLEDGMENTS

We acknowledge the assistance of Yufeng Cai, Vincent Chou, Madhavi Kolli, Anik Peeters, Madhavi Nalam, and Claire Baldwin in the acquisition of data and the preparation of the manuscript. Data were collected in part with the help of Nicholas Sauter at the Advanced Light Source at the Lawrence Berkeley National Laboratory.

TMC114 was provided by Tibotec and Amprenavir was provided by GlaxoSmithKline. The MDR protease gene was provided by Sepracor, Inc.

This research was supported by the National Institutes of Health (NIH), grant P01-GM66524, and Tibotec/COSAT. N.M.K. was supported by NIH grant F32-GM62993.

REFERENCES

1. **Ala, P. J., E. E. Huston, R. M. Klabe, P. K. Jadhav, P. Y. Lam, and C. H. Chang.** 1998. Counteracting HIV-1 protease drug resistance: structural analysis of mutant proteases complexed with XV638 and SD146, cyclic urea amides with broad specificities. Biochemistry **37:**15042–15049.
2. **Arasteh, K., A. Clumeck, H. Pozniak, H. Jäger, M. De Pauw, H. Müller, M. Peeters, R. Hoetelmans, S. De Meyer, I. Van der Sandt, S. Comhaire, and R. Van der Geest.** 2003. First clinical results on antiretroviral activity, pharmacokinetics, and safety of TMC114, an HIV-1 protease inhibitor, in multiple PI-experienced patients, abstr. 8. 10th Conference on Retroviruses and Opportunistic Infections (CROI), Boston, Mass.
3. **Baldwin, E. T., T. N. Bhat, B. Liu, N. Pattabiraman, and J. W. Erickson.** 1995. Structural basis of drug resistance for the V82A mutant of HIV-1 proteinase. Nat. Struct. Biol. **2:**244–249.
4. **Brünger, A. T., P. D. Adams, G. M. Clore, W. L. DeLano, P. Gros, R. W. Grosse-Kunstleve, J. S. Jiang, J. Kuszewski, M. Nilges, N. S. Pannu, R. J. Read, L. M. Rice, T. Simonson, and G. L. Warren.** 1998. Crystallography & NMR system: a new software suite for macromolecular structure determination. Acta Crystallogr. D Biol. Crystallogr. **54:**905–921.

5. **Chapman, M. S.** 1995. Restrained real-space macromolecular refinement using a new resolution-dependent electron density function. Acta Crystallogr. A **51:**69–80.
6. **Chou, K.-C., A. G. Tomasselli, I. M. Reardon, and R. L. Heinrikson.** 1996. Predicting human immunodeficiency virus protease cleavage sites in proteins by a discriminant function method. Proteins **24:**51–72.
7. **Coffin, J. M.** 1995. HIV population dynamics in vivo: implications for genetic variation, pathogenesis and therapy. Science **257:**483–489.
8. **Collaborative Computational Project Number.** 1994. The CCP4 suite: programs for protein crystallography. Acta Crystallogr. D Biol. Crystallogr. **50:**760–763.
9. **Condra, J. H., W. A. Schleif, O. M. Blahy, L. J. Gabryelski, D. J. Graham, J. C. Quintero, A. Rhodes, H. L. Robbins, E. Roth, M. Shivaprakash, D. Titus, T. Yang, H. Teppler, K. E. Squires, P. J. Deutsch, and E. Emini.** 1995. In vivo emergence of HIV-1 variants resistant to multiple protease inhibitors. Nature **374:**569–571.
10. **de Béthune, M.-P., P. Wigerinck, H. Jonckheere, A. Tahri, L. Maes, R. Pauwels, and J. Erickson.** 2001. TMC 114, a very potent protease inhibitor (PI) with an excellent profile against HIV variants highly resistant to current PI's, abst. F-1677. 41st International Conference on Antimicrobial Agents and Chemotherapy, Chicago, Ill.
11. **Debouck, C.** 1992. The HIV-1 protease as a therapeutic target for AIDS. AIDS Res. Hum. Retrovir. **8:**153–164.
12. **De Meyer, S., H. Van Marck, J. Veldeman, P. McKenna, R. Pauwels, and M.-P. de Béthune.** 2003. Antiviral activity of TMC114, a potent next-generation PI, against >4000 recent recombinant clinical isolates exhibiting a wide range of (PI) resistance profiles, abst. 17. XII International HIV Drug Resistance Workshop, Los Cabos, Mexico.
13. **De Meyer, S., H. Azijn, M. Van Ginderen, I. De Baere, R. Pauwels, and M.-P. de Béthune.** 2002. In vitro selection experiments demonstrate an increased genetic barrier to resistance development to TMC114 as compared with currently licensed PIs, abst. 5. XI International HIV Drug Resistance Workshop, Seville, Spain.
14. **Doyon, L., G. Croteau, D. Thibeault, F. Poulin, L. Pilote, and D. Lamarre.** 1996. Second locus involved in human immunodeficiency virus type 1 resistance to protease inhibitors. J. Virol. **70:**3763–3769.
15. **Ferrin, T. E., C. C. Huang, L. E. Jarvis, and R. Langridge.** 1988. The MIDAS display system. J. Mol. Graph. **6:**13–27.
16. **Ghosh, A., W. Thompson, P. Fitzgerald, J. Culberson, M. Axel, S. McKee, J. Huff, and P. Anderson.** 1994. Structure-based design of HIV-1 protease inhibitors: replacement of two amides and a 10 pi-aromatic system by a fused bis-tetrahydrofuran. J. Med. Chem. **37:**2506–2508.
17. **Henderson, L. E., T. D. Copeland, R. C. Sowder, A. M. Schultz, and S. Oraszlan.** 1988. Human retroviruses, cancer and AIDS: approaches to prevention and therapy. Liss, New York, N.Y.
18. **Jones, T. A., M. Bergdoll, and M. Kjeldgaard.** 1990. O: A macromolecular modeling environment, p. 189–195. *In* C. Bugg and S. Ealick (ed.), Crystallographic and modeling methods in molecular design. Springer-Verlag Press, Berlin, Germany.
19. **Kim, E. E., C. T. Baker, M. D. Dwyer, M. A. Murcko, et al.** 1995. Crystal structure of HIV-1 protease in complex with vx-478, a potent and orally bioavailable inhibitor of the enzyme. J. Am. Chem. Soc. **117:**1181–1182.
20. **King, N. M., L. Melnick, M. Prabu-Jeyabalan, E. A. Nalivaika, S.-S. Yang, Y. Gao, X. Nie, C. Zepp, D. L. Heefner, and C. A. Schiffer.** 2002. Lack of synergy for inhibitors targeting a multi-drug-resistant HIV-1 protease. Protein Sci. **11:**418–429.

20a. **King, N. M., M. Prabu-Jeyabalan, E. A. Nalivaika, and C. A. Schiffer.** 2004. Combatting susceptibility to drug-resistance: Lessons from HIV-1 protease. Chem. Biol., in press.

21. **La Seta Catamancio, S., M. P. De Pasquale, P. Citterio, S. Kurtagic, M. Galli, and S. Rusconi.** 2001. In vitro evolution of the human immunodeficiency virus type 1 Gag-protease region and maintenance of reverse transcriptase resistance following prolonged drug exposure. J. Clin. Microbiol. **39:**1124–1129.
22. **Markowitz, M., H. Mo, D. J. Kempf, D. W. Norbeck, T. N. Bhat, J. W. Erickson, and D. D. Ho.** 1995. Selection and analysis of human immunodeficiency virus type 1 variants with increased resistance to ABT-538, a novel protease inhibitor. J. Virol. **69:**701–706.
23. **Minor, W.** 1993. XDISPLAYF program. Purdue University, West Lafayette, Ind.
24. **Morris, R. J., A. Perrakis, and V. S. Lamzin.** 2002. ARP/wARP's model-building algorithms. I. The main chain. Acta Crystallogr. D Biol. Crystallogr. **58:**968–975.
25. **Munshi, S., Z. Chen, Y. Yan, Y. Li, D. Olsen, H. Schock, B. Galvin, B. Dorsey, and L. Kuo.** 2000. An alternate binding site for the P1-P3 group of a class of potent HIV-1 protease inhibitors as a result of concerted structural change in the 80s loop of the protease. Acta Crystallogr. D. Biol. Crystallogr. **56:**381–388.
26. **Murshudov, G. N., A. A. Vagin, and E. J. Dodson.** 1997. Refinement of macromolecular structures by the maximum-likelihood method. Acta Crystallogr. D Biol. Crystallogr. **53:**240–255.
27. **Navaza, J.** 1994. AMoRe: an automated package for molecular replacement. Acta Crystallogr. A **50:**157–163.
28. **Nicholls, A., K. Sharp, and B. Honig.** 1991. Protein folding and association: insights from the interfacial and thermodynamic properties of hydrocarbons. Proteins **11:**281–296.
29. **Ohtaka, H., A. Velazquez-Campoy, D. Xie, and E. Freire.** 2002. Overcoming drug resistance in HIV-1 chemotherapy: the binding thermodynamics of amprenavir and TMC-126 to wild-type and drug-resistant mutants of the HIV-1 protease. Protein Sci. **11:**1908–1916.
30. **Otwinowski, Z., and W. Minor.** 1997. Processing of X-ray diffraction data collected in oscillation mode. Methods Enzymol. **276:**307–326.
31. **Pazhanisamy, S., J. Partaledis, B. Rao, and D. Livingston.** 1998. In vitro selection and characterization of VX-478 resistant HIV-1 variants. Adv. Exp. Med. Biol. **436:**75–83.
32. **Pettit, S. C., N. Sheng, R. Tritch, S. Erickson-Vitanen, and R. Swanstrom.** 1998. The regulation of sequential processing of HIV-1 Gag by the viral protease. Adv. Exp. Med. Biol. **436:**15–25.
33. **Prabu-Jeyabalan, M., E. Nalivaika, and C. A. Schiffer.** 2000. How does a symmetric dimer recognize an asymmetric substrate? A substrate complex of HIV-1 protease. J. Mol. Biol. **301:**1207–1220.
34. **Prabu-Jeyabalan, M., E. A. Nalivaika, N. M. King, and C. A. Schiffer.** 2003. Viability of a drug-resistant HIV-1 protease variant: structural insights for better anti-viral therapy. J. Virol. **77:**1306–1315.
35. **Prabu-Jeyabalan, M., E. A. Nalivaika, and C. A. Schiffer.** 2002. Substrate shape determines specificity of recognition for HIV-1 protease: analysis of crystal structures of six substrate complexes. Structure **10:**369–381.
36. **Roberts, N. A.** 1995. Drug-resistance patterns of saquinavir and other HIV proteinase inhibitors. AIDS **9**(Suppl. 2)**:**S27-S32.
37. **Rose, J. R., R. Salto, and C. S. Craik.** 1993. Regulation of autoproteolysis of the HIV-1 and HIV-2 proteases with engineered amino acid substitutions. J. Biol. Chem. **268:**11939–11945.
38. **Schock, H., V. Garsky, and L. Kuo.** 1996. Mutational anatomy of an HIV-1 protease variant conferring cross-resistance to protease inhibitors in clinical trials. Compensatory modulations of binding and activity. J. Biol. Chem. **271:**31957–31963.
39. **Shafer, R. W., P. Hsu, A. K. Patick, C. Craig, and V. Brendel.** 1999. Identification of biased amino acid substitution patterns in human immunodeficiency virus type 1 isolates from patients treated with protease inhibitors. J. Virol. **73:**6197–6202.
40. **Shafer, R. W., D. Stevenson, and B. Chan.** 1999. Human immunodeficiency virus reverse transcriptase and protease sequence database. Nucleic Acids Res. **27:**348–352.
41. **Sigurskjold, B.** 2000. Exact analysis of competition ligand binding by displacement isothermal titration calorimetry. Anal. Biochem. **277:**260–266.
42. **Todd, M. J., I. Luque, A. Velazquez-Campoy, and E. Freire.** 2000. Thermodynamic basis of resistance to HIV-1 protease inhibition: calorimetric analysis of the V82F/I84V active site resistant mutant. Biochemistry **39:**11876–11883.
43. **Valzaquez-Campoy, A., Y. Kiso, and E. Freire.** 2001. The binding energetics of first- and second-generation HIV-1 protease inhibitors: implications for drug design. Arch. Biochem. Biophys. **390:**169–175.
44. **Wlodawer, A., and J. W. Erickson.** 1993. Structure-based inhibitors of HIV-1 protease. Annu. Rev. Biochem. **62:**543–585.
45. **Yoshimura, K., R. Kato, M. Kavlick, A. Nguyen, V. Maroun, K. Maeda, K. Hussain, A. Ghosh, S. Gulnik, J. Erickson, and H. Mitsuya.** 2002. A potent human immunodeficiency virus type 1 protease inhibitor, UIC-94003 (TMC-126), and selection of a novel (A28S) mutation in the protease active site. J. Virol. **76:**1349–1358.
46. **Zhang, Y. M., H. Imamichi, T. Imamichi, H. C. Lane, J. Falloon, M. B. Vasudevachari, and N. P. Salzman.** 1997. Drug resistance during indinavir therapy is caused by mutations in the protease gene and in its Gag substrate cleavage sites. J. Virol. **71:**6662–6670.